Radiatively broken symmetries of nonhierarchical neutrinos

Amol Dighe,[1] Srubabati Goswami,[2] and Probir Roy[1]

[1] *Tata Institute of Fundamental Research, Homi Bhabha Road, Mumbai 400 005, India*

[2] *Harish-Chandra Research Institute, Chhatnag Road, Jhusi, Allahabad 211 019, India*

Abstract

Symmetry-based ideas, such as the quark-lepton complementarity (QLC) principle and the tribimaximal mixing (TBM) scheme, have been proposed to explain the observed mixing pattern of neutrinos. We argue that such symmetry relations need to be imposed at a high scale $\Lambda \sim 10^{12}$ GeV characterizing the large masses of right-handed neutrinos required to implement the seesaw mechanism. For nonhierarchical neutrinos, renormalisation group evolution down to a laboratory energy scale $\lambda \sim 10^3$ GeV tends to radiatively break these symmetries at a significant level and spoil the mixing pattern predicted by them. However, for Majorana neutrinos, suitable constraints on the extra phases $\alpha_{2,3}$ enable the retention of those high scale mixing patterns at laboratory energies. We examine this issue within the Minimal Supersymmetric Standard Model (MSSM) and demonstrate the fact posited above for two versions of QLC and two versions of TBM. The appropriate constraints are worked out for all these four cases. Specifically, a preference for $\alpha_2 \approx \pi$ (i.e. $m_1 \approx -m_2$) emerges in each case. We also show how a future accurate measurement of θ_{13} may enable some discrimination among these four cases in spite of renormalization group evolution.

PACS numbers: 11.10.Hi, 12.15.Ff, 14.60.Pq

Keywords: neutrino masses and mixing, renormalisation group running, quark-lepton complementarity, tribimaximal mixing

I. INTRODUCTION

Outstanding recent experiments have increased our knowledge [1] of neutrino masses and mixing angles enormously. We are already certain that at least two of the three known neutrinos are massive, the heavier and the lighter of them being respectively $\gtrsim 0.05$ eV and $\gtrsim 0.009$ eV in mass. We also know that two of the three neutrino mixing angles are large: $\theta_{23} \approx 45^\circ$ and $\theta_{12} \approx 34^\circ$, while the third is significantly smaller: $\theta_{13} < 12^\circ$. The total sum of the neutrino masses is also cosmologically bounded from above by $\mathcal{O}(1)$ eV. Much remains to be known, though. The values of θ_{13} and the leptonic CP violating Dirac phase δ_ℓ, are still unknown. So is the ordering of the neutrino masses m_i $(i = 1, 2, 3)$ – whether it is normal ($|m_3| > |m_{1,2}|$) or inverted ($|m_3| < |m_{1,2}|$). We also do not know if the three neutrinos are hierarchically spaced in mass like charged fermions or if they are nonhierarchical. Our term nonhierarchical here includes both the inverted hierarchical (IH) case , i.e $|m_3| \ll |m_1| \sim |m_2| \sim 0.05$ eV, and the quasi-degenerate (QD) situation [3], i.e. $|m_1| \sim |m_2| \sim |m_3| \gg 0.05$ eV, the latter with either a normal or an inverted mass ordering. Neither of these scenarios is observationally excluded as yet and we focus on them. As per our present knowledge, the average neutrino mass could still in fact be anywhere between half of the atmospheric oscillation mass scale, i.e. ≈ 0.025 eV and a third of the cosmological upper bound, i.e. ≈ 0.3 eV. Finally, most theoretical ideas expect the three neutrinos to be Majorana particles whose masses m_i can be complex. In that case, since one of their phases can be rotated away, there are two additional, possibly nonzero, phases [2] on which we do not have any direct information at present. This is because no convincing evidence exists as yet of neutrinoless nuclear double beta decay which is the only known direct probe [4] on these phases. Indirectly, of course, some constraints on these phases may also arise from considerations of leptogenesis [5]. It is nevertheless worthwhile to try to constrain these phases in some other way. That is one of the aims of the present work, which is an elaboration of our earlier shorter communication [6] with many additional results. In particular, we demonstrate here that, given the constraints on these Majorana phases, a measurement of θ_{13} can make some discrimination among four scenarios considered by us despite renormalization group (RG) running.

The observed bilarge pattern of neutrino mixing has led to the idea of some kind of a

symmetry at work. Several symmetry-based relations[1] have in fact been proposed, which give rise to specific neutrino mixing patterns. Two of the most promising mixing patterns, that we will be concerned with here, are (i) quark-lepton complementarity (QLC) [7, 8, 9, 10, 11] and (ii) tribimaximal mixing (TBM) [12]. QLC involves bimaximal mixing [13] followed by the unitary transformation of quark mixing. A bimaximal mixing can in turn be generated by a μ-τ exchange symmetry [14], an $L_\mu - L_\tau$ gauge symmetry [15], or an S_3 permutation symmetry [16]. The second step is inspired by SU(5) or SO(10) GUT, as discussed later. Similarly, a tribimaximal mixing pattern may be obtained from an A_4 [17] or S_3 [18] family symmetry. However, a major issue in connection with such symmetries is the scale at which they are to be implemented. Neutrino masses and mixing angles are related directly to the corresponding Yukawa coupling strengths which run with the energy scale. There is as yet no universally accepted explanation of the origin of neutrino masses, but the seesaw mechanism [19] is the most believable candidate so far. The form of the light neutrino mass matrix in family space in that case is $\mathcal{M}_\nu = -(m_\nu^D)^T M_R^{-1} m_\nu^D$, where m_ν^D is the Dirac neutrino mass matrix (analogous to the charged fermion ones) and M_R the mass matrix for very heavy right chiral singlet neutrinos. If the Dirac mass of the heaviest neutrino is taken to be 1 – 100 GeV, the atmospheric neutrino data require typical eigenvalues of M_R to be in the 10^{11}–10^{15} GeV range [20]. This is also the desirable magnitude for M_R from the standpoint of a successful leptogenesis [21]. From these considerations, we choose to implement the above mentioned symmetries at the scale $\Lambda \sim 10^{12}$ GeV. One can take issue with the particular value chosen for Λ. However, our conclusions are only logarithmically sensitive to the precise value of this scale.

A question arises immediately on the application of such a high scale symmetry on the elements of the neutrino mass matrix. It concerns their radiative breaking via RG evolution down to a laboratory energy scale $\lambda \sim 10^3$ GeV. The actual evolution [22, 23, 24] needs to be worked out in a specific theory which we choose to be the minimal supersymmetric standard model (MSSM [25]). That is why we have taken λ to be of the order of the explicit supersymmetry breaking or the intra-supermultiplet splitting scale $\mathcal{O}$(TeV). Once again, our calculations are only logarithmically sensitive to this exact choice. The point, however, is

[1] Here one should perhaps make a distinction between a symmetry of the Lagrangian and just a special relation among coupling strengths or masses. Nevertheless, the relations of concern to us can be implemented through specific symmetries of the Lagrangian.

that – for nonhierarchical neutrinos – symmetry relations formulated at Λ will in general get spoilt on evolution down to λ.

The full RG equations for the evolution of neutrino masses and mixing angles in the MSSM have been worked out [23, 24] in detail. In particular, the evolution effects on the mixing angles are found to be controlled by the quantities [6] $\Delta_\tau |m_i + m_j|^2/(|m_i|^2 - |m_j|^2)$ where Δ_τ, to be specified later, is a small fraction $\lesssim 10^{-2}$, while i, j refer to the concerned neutrino mass eigenstates. Consequently, these effects are negligible for a normal hierarchical mass pattern with $|m_3| \gg |m_2| \gg |m_1|$. RG effects can become significantly large only when neutrinos are nonhierarchical. There is another important characteristic of the above-mentioned ratios. While their denominators involve only the absolute masses $|m_i|$, the numerators involve the combinations $|m_i + m_j|^2$. Therefore, with appropriate constraints on the neutrino Majorana phases, the desired symmetry relations can be approximately preserved at the laboratory scale λ even for nonhierarchical neutrinos – in agreement with the mixing pattern that has emerged from the oscillation data. The constraints on the majorana phases and the consequent discrimination among the scenaios by a measurement of θ_{13} constitute our main results. Our work is somewhat complementary to that of Ref. [26] in the QLC sector and Ref. [27] in the TBM sector.

In this paper we work out in detail the last-mentioned constraints on the neutrino Majorana phases in the (i) bimaximal mixing + QLC and (ii) TBM scenarios respectively. Each of these comes in two variations. So we have in all four cases at hand. Thus, the scope of the present work is much larger than our earlier shorter communication [6] which addressed only one version of QLC and did not consider the implications for θ_{13}. A major technical observation utilized by us is the following. Suppose θ_{13}^Λ, the high scale value of the angle θ_{13}, is sufficiently small (as is the case for the situations considered here) such that $\mathcal{O}(\theta_{13})$ terms can be neglected in comparison with other $\mathcal{O}(1)$ terms in the RG equations [24]. Then the neutrino mass matrix $\mathcal{M}_\nu^\lambda$, at the laboratory scale λ, becomes analytically tractable in terms of its high scale form $\mathcal{M}_\nu^\Lambda$. In fact, the relation obtained looks quite simple and transparent. The step from there to explicit constraints on the neutrino Majorana phases is then shown to be quite straightforward. The rest of this paper is organised as follows. Sec. II contains a description of the parametrisation that we find convenient to adopt for nonhierarchical neutrino masses. In Sec. III, we introduce two versions each of the QLC and TBM scenarios to be implemented at the high scale. In sec. IV, we discuss the energywise downward evolution

of the Pontecorvo-Maki-Nakagawa-Sakata (PMNS) mixing matrix in general, and its effects on the predictions of the scenarios under consideration. In sec. V we study the constraints on neutrino and MSSM parameters in order for the scanarios to be valid and explore if these scenarios may be distinguished by means of more accurate measurements of the neutrino mixing angles. The concluding sec. VI consists of a summary and the discussion of our main results.

II. PARAMETRISATION OF NONHIERARCHICAL NEUTRINO MASSES

We work in the convention [28] in which the neutrino mass eigenstates $|\nu_1\rangle, |\nu_2\rangle, |\nu_3\rangle$ are related to the flavour eigenstates $|\nu_e\rangle, |\nu_\mu\rangle, |\nu_\tau\rangle$ with the unitary mixing matrix U_ν:

$$|\nu_\alpha\rangle = U_{\alpha i}|\nu_i\rangle \ , \tag{1}$$

α and i being flavour and mass indices respectively. We take the neutrino mass term in the Lagrangian to be

$$\mathcal{L}^\nu_{\rm mass} = -\frac{1}{2}\overline{\nu^C_{L\alpha}}\mathcal{M}_{\nu\alpha\beta}\nu_{L\beta} + h.c. \tag{2}$$

Thus,

$$U^\dagger_\nu \mathcal{M}_\nu U^*_\nu = \begin{pmatrix} m_1 & 0 & 0 \\ 0 & m_2 & 0 \\ 0 & 0 & m_3 \end{pmatrix} \ , \tag{3}$$

where m_i are in general complex. However, one of the three phases of $m_{1,2,3}$ can be absorbed in the overall phase choice of ν_L in (2). We can therefore choose

$$m_1 = |m_1| \ , \ m_2 = |m_2|e^{i\alpha_2} \ , \ m_3 = |m_3|e^{i\alpha_3} \ , \tag{4}$$

where $\alpha_{2,3}$ are real. Experiments with atmospheric neutrinos tell us that [28, 29]

$$|\delta m^2_A| \equiv ||m_3|^2 - |m_{2,1}|^2| = (2.4 \pm 0.3) \times 10^{-3} \ \text{eV}^2 \ , \tag{5}$$

while experiments with solar electron neutrinos and reactor electron antineutrinos yield [28, 29]

$$\delta m^2_S \equiv |m_2|^2 - |m_1|^2 = (7.9 \pm 0.4) \times 10^{-5} \ \text{eV}^2 \ . \tag{6}$$

For charged fermions ($f = u, d, l$), the mass term is

$$\mathcal{L}^f_{\rm mass} = -\frac{1}{2}\overline{f_{R\alpha}}m_{f\alpha\beta}f_{L\beta} + h.c. \tag{7}$$

The corresponding mass matrix m_f is put into a diagonal form by

$$U_f^\dagger m_f^\dagger m_f U_f = |m_f^{(D)}|^2 \; . \tag{8}$$

Now the unitary Cabbibo-Kobayashi-Maskawa (CKM) and the Pontecorvo-Maki-Nakagawa-Sakata (PMNS) mixing matrices, whose elements contribute to the observed quark and neutrino processes respectively, are given by

$$\begin{aligned} V_{\rm CKM} &= U_u^\dagger U_d \; , \\ U_{\rm PMNS} &= U_\ell^\dagger U_\nu \; . \end{aligned} \tag{9}$$

One can write $U_{\rm PMNS}$ in the standard basis [28] in terms of the angles $\theta_{12}, \theta_{23}, \theta_{13}$ and the CP violating phase δ_ℓ. With $s_{ij} \equiv \sin\theta_{ij}$ and $c_{ij} \equiv \cos\theta_{ij}$,

$$U_{\rm PMNS} = \begin{pmatrix} c_{12}c_{13} & s_{12}c_{13} & s_{13}e^{-i\delta_\ell} \\ -s_{12}c_{23} - c_{12}s_{23}s_{13}e^{i\delta_\ell} & c_{12}c_{23} - s_{12}s_{23}s_{13}e^{i\delta_\ell} & s_{23}c_{13} \\ s_{12}s_{23} - c_{12}c_{23}s_{13}e^{i\delta_\ell} & -c_{12}s_{23} - s_{12}c_{23}s_{13}e^{i\delta_\ell} & c_{23}c_{13} \end{pmatrix} \; . \tag{10}$$

The experiments mentioned earlier then also tell us that [28, 29]

$$\begin{aligned} \theta_{12} &= 33.9^\circ \pm 1.6^\circ \; , \\ \theta_{23} &= 43.3^\circ \pm 8.2^\circ \; , \\ \theta_{13} &< 12^\circ \; . \end{aligned} \tag{11}$$

We find it convenient to parametrise the absolute masses $|m_i|$ for nonhierarchical neutrinos in terms of three real parameters m_0, ρ_A and ϵ_S as follows:

$$\begin{aligned} |m_1| &= m_0(1-\rho_A)(1-\epsilon_S) \; , \\ |m_2| &= m_0(1-\rho_A)(1+\epsilon_S) \; , \\ |m_3| &= m_0(1+\rho_A) \; . \end{aligned} \tag{12}$$

In eqs. (12), m_0 defines the overall mass scale of the neutrinos, whereas ρ_A and ϵ_S are dimensionless fractions with $-1 \leq \rho_A \ll 1$ and $0 < \epsilon_S < |\rho_A|$ for nonhierarchical neutrinos. The sign of ρ_A is positive (negative) for a normal (inverted) ordering of neutrino masses. Moreover, $\rho_A \approx -1$ ($|\rho_A| \ll 1$) for the IH (QD) case; in either case $\epsilon_S \ll 1$. For comparison,

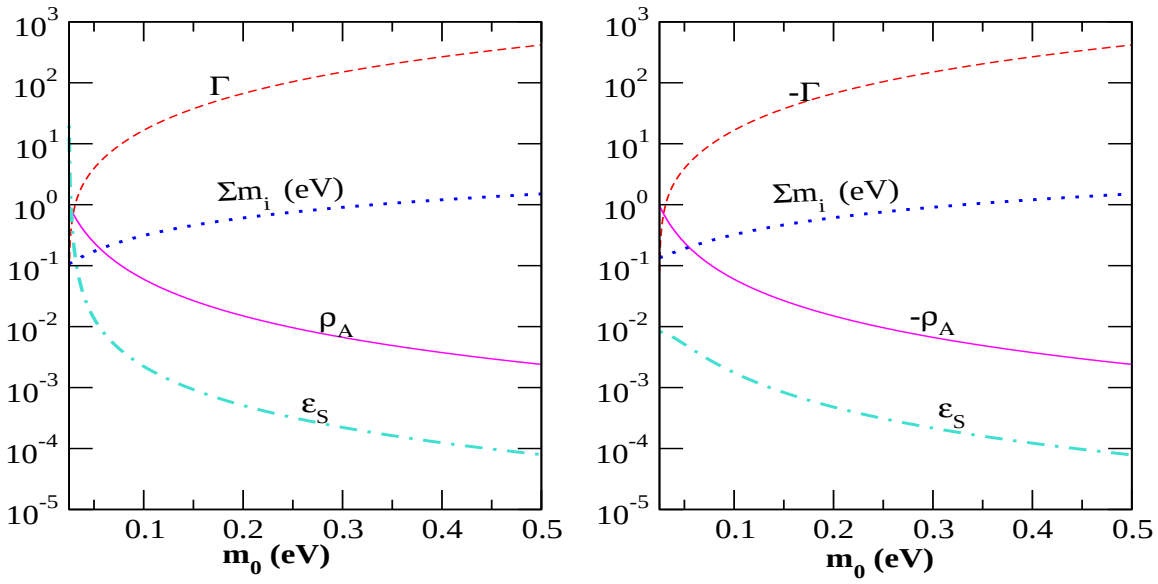

FIG. 1: The parameters ρ_A, ϵ_S and Γ as well as the value of $\sum |m_i|$ (eV) as functions of m_0, for a normal (left panel) and an inverted (right panel) mass ordering of neutrinos. Note that ρ_A and Γ are negative for inverted mass ordering. For normal ordering, ϵ_S goes to near unity with low m_0.

it may be noted that for normally hierarchical neutrinos, $\rho_A \sim \epsilon_S \sim 1$. We can further write the solar and atmospheric neutrino mass squared differences as

$$\begin{aligned} \delta m^2_S &= |m_2|^2 - |m_1|^2 \approx 4m_0^2(1-\rho_A)^2\epsilon_S \ , \\ |\delta m^2_A| &= ||m_3|^2 - (|m_1|/2 + |m_2|/2)^2| = 4m_0^2|\rho_A| \ . \end{aligned} \tag{13}$$

Utilizing (6), (5) and (13), we see that

$$m_0 > 0.024 \text{ eV} \ . \tag{14}$$

Also, the cosmologically bounded sum of neutrino absolute masses is given by

$$\Sigma_i |m_i| = 3\, m_0(1-\rho_A/3) \lesssim 1 \text{ eV} \ . \tag{15}$$

From (13) and (15), it follows that

$$\frac{4}{9}\frac{(\sum |m_i|)^2}{|\delta m^2_A|} = \frac{(1-\rho_A/3)^2}{|\rho_A|} \ . \tag{16}$$

Utilising (5), (16) and the cosmological upper bound (15), we get $|\rho_A| \gtrsim 5.5 \times 10^{-3}$.

In Fig.1, we show how ρ_A, ϵ_S and $\sum |m_i|$ behave as functions of m_0. We also find it convenient to define the derived dimensionless parameter

$$\Gamma \equiv \frac{1}{\rho_A} - \rho_A \ , \tag{17}$$

whose behaviour is included in the figure. Since $|\rho_A| < 1$, the sign of Γ is positive ($\rho_A > 0$) for a normal ordering and negative ($\rho_A < 0$) for an inverted ordering of the neutrino masses. The inequality $5.5 \times 10^{-3} \lesssim |\rho_A| < 1$ translates to $|\Gamma| \lesssim 180$. We can generate typical numbers for nonhierarchical neutrinos: In the IH scenario, for instance, if m_0 is chosen as 0.025 eV, we get $\rho_A \approx -1$, $\Gamma \approx 0^-$, and $\epsilon_S \approx 8 \times 10^{-3}$. On the other hand, for QD neutrinos, choosing $m_0 = 0.2$ eV, we have $|\rho_A| \approx 1.5 \times 10^{-2}$, $|\Gamma| \approx 65$, and $\epsilon_S \approx 5 \times 10^{-4}$.

III. SYMMETRIES AND MIXING ANGLES AT THE HIGH SCALE

The neutrino mass matrix at the high scale Λ originates from a dimension-5 operator

$$\mathcal{O} = c_{\alpha\beta} \frac{(\ell_\alpha . H)(\ell_\beta . H)}{\Lambda} \, . \tag{18}$$

In (18), ℓ_α and H are the SU(2) doublet lepton and Higgs fields respectively and $c_{\alpha\beta}$ are dimensionless coefficients that run with the energy scale. Then

$$\mathcal{M}^{\Lambda}_{\nu\alpha\beta} \sim c_{\alpha\beta} \frac{v^2}{\Lambda} \, , \tag{19}$$

where $v = 246$ GeV and $\Lambda \sim M_{\rm MAJ}$, the Majorana mass characterising the heavy SM-singlet Majorana neutrino N. The symmetries at the high scale Λ give rise to specific structures for the matrix $\mathcal{M}^{\Lambda}_{\nu}$, and hence predict the values of the mixing angles θ^{Λ}_{ij} at the scale Λ. There is an issue about a consistent definition of $\nu_{1,2}$ at all scales. Solar neutrino experiments tell us that $|m^{\lambda}_2| > |m^{\lambda}_1|$, where λ is the laboratory scale. We *define* ν_1 and ν_2 at higher scales in a way such that $|m_2| \geq |m_1|$ at *all* scales, and in particular, $|m^{\Lambda}_2| > |m^{\Lambda}_1|$.

In this section, we introduce four different symmetries and the corresponding predictions on the neutrino mixing angles at this high scale:

A. QLC1

Quark-lepton complementarity [7, 8, 9, 10, 11] links the difference between the measured and the maximal (i.e. 45°) values of the neutrino mixing angle θ_{12} to the Cabbibo angle $\theta_c = 12.6^\circ \pm 0.1^\circ$ [28]. We first follow a particular basis independent formulation "QLC1"

[9] of this principle [2]:

$$U_{\rm PMNS} = V_{\rm CKM}^{\dagger} U_{\nu,\rm bm} \ , \tag{20}$$

where $U_{\nu,\rm bm}$ is the specific bimaximal form [13] for the unitary neutrino mixing matrix. Eq. (20) gives rise to the "QLC1" relation [3]

$$\theta_{12}^{\Lambda} + \frac{\theta_c}{\sqrt{2}} = \frac{\pi}{4} + \mathcal{O}(\theta_c^3) \ . \tag{21}$$

The identification of (20) as a statement of QLC becomes more transparent in the basis with $U_u = I$, i.e. where the matrix $Y_u^{\dagger} Y_u$ is diagonal. It follows from (9) that $V_{CKM} = U_d$ in this basis. Now a comparison of (9) and (20), together with the assumption of U_ν being $U_{\nu,\rm bm}$, yields the SU(5) GUT-inspired quark-lepton symmetry relation $U_d = U_l$. Eq. (20), as it stands, is basis independent, however.

Eq. (20) yields the neutrino mixing angles at the high scale Λ to be

$$\begin{aligned} \theta_{12}^{\Lambda} &= \frac{\pi}{4} - \frac{\theta_c}{\sqrt{2}} + \mathcal{O}(\theta_c^3) \approx 35.4^{\circ} \\ \theta_{23}^{\Lambda} &= \frac{\pi}{4} - |V_{cb}| - \frac{\theta_c^2}{4} + \mathcal{O}(\theta_c^3) \approx 42.1^{\circ} \ , \\ \theta_{13}^{\Lambda} &= \frac{\theta_c}{\sqrt{2}} + \mathcal{O}(\theta_c^3) \approx 8.9^{\circ} \ . \end{aligned} \tag{22}$$

Thus, QLC1 predicts a value of θ_{13}^{Λ} that is close to the current experimental bound.

B. QLC2

In a second version of quark-lepton complementarity, "QLC2" [8, 9] , one assumes a bimaximal structure for the charged lepton mixing matrix, $U_\ell = U_{\ell,\rm bm}$ and the form

$$U_{\rm PMNS} = U_{\ell,\rm bm} V_{\rm CKM}^{\dagger} \ , \tag{23}$$

for the PMNS matrix. Eq. (23) yields in a straightforward way the relation

$$\theta_{12}^{\Lambda} + \theta_c = \frac{\pi}{4} + \mathcal{O}(\theta_c^3) \ . \tag{24}$$

[2] There could be a more general statement of QLC1 with an additional diagonal phase matrix Γ_δ between $V_{\rm CKM}^{\dagger}$ and $U_{\nu,\rm bm}$. But for consistency and simplicity, we choose eq. (20).

[3] We do not distinguish between θ_c^{Λ} and θ_c^{λ} since the running of θ_c is negligible on account of the hierarchical nature of quarks belonging to different generations.

One may note that, in the basis with $U_d = I$, i.e. where $Y_d^\dagger Y_d$ is diagonal, (23) yields the SO(10) GUT-inspired relation $U_u = U_\nu$.

Eq. (23) leads to the following values for the nautrino mixing angles at the high scale:

$$\begin{aligned}
\theta_{12}^\Lambda &= \frac{\pi}{4} - \theta_c + \mathcal{O}(\theta_c^3) \approx 32.4^\circ \ , \\
\theta_{23}^\Lambda &= \frac{\pi}{4} - \frac{|V_{cb}|}{\sqrt{2}} + \mathcal{O}(\theta_c^3) \approx 43.4^\circ \ , \\
\theta_{13}^\Lambda &= \frac{|V_{cb}|}{\sqrt{2}} + \mathcal{O}(\theta_c^3) \approx 1.6^\circ \ .
\end{aligned} \tag{25}$$

The value of θ_{13}^Λ predicted in QLC2 is beyond the measuring capacity of the neutrino experiments planned during the next decade.

C. TBM1

The tribimaximal form of the neutrino mixing matrix is given by

$$U_{\nu,\mathrm{tbm}}^\Lambda = \frac{1}{\sqrt{6}} \begin{pmatrix} 2 & \sqrt{2} & 0 \\ -1 & \sqrt{2} & \sqrt{3} \\ 1 & -\sqrt{2} & \sqrt{3} \end{pmatrix} = R_{23}(\frac{\pi}{4}) R_{13}(0) R_{12}(\sin^{-1}\frac{1}{\sqrt{3}}) \ . \tag{26}$$

In the standard TBM scenario [12], which we refer to as TBM1, one has $U_{\mathrm{PMNS}}^\Lambda = U_\nu^\Lambda$ since the charged lepton mass matrix at the high scale is already flavour diagonal. Then we have

$$\theta_{12}^\Lambda \approx 35.3^\circ \ , \ \theta_{23}^\Lambda = 45^\circ \ , \ \theta_{13}^\Lambda = 0^\circ \ . \tag{27}$$

D. TBM2

Small deviations from the tribimaximal scenario TBM1 above have been considered in the literature [34, 35], where the deviation originates from the mixing in the charged lepton sector. Here we consider the version in Ref. [34], and call it TBM2. Here $U_{\mathrm{PMNS}} = V_{\ell\mathrm{L}}^\dagger U_{\nu,\mathrm{tbm}}$, where $V_{\ell L}$ has the form [11]

$$V_{\ell L} = \begin{pmatrix} 1 & \theta_c/3 & 0 \\ \theta_c/3 & 1 & -|V_{cb}| \\ 0 & |V_{cb}| & 1 \end{pmatrix} + \mathcal{O}(\theta_c^3) \ , \tag{28}$$

with the factor of 1/3 coming from the Georgi-Jarlskog relation [36] $m_\mu/m_s = 3$ at the GUT scale. As a result, we have at the high scale

$$\begin{aligned}
\theta_{12}^\Lambda &= \sin^{-1}\frac{1}{\sqrt{3}} - \frac{\theta_c}{3\sqrt{2}} + \mathcal{O}(\theta_c^3) \approx 32.3^\circ \ , \\
\theta_{23}^\Lambda &= \frac{\pi}{4} - |V_{cb}| + \mathcal{O}(\theta_c^3) \approx 42.7^\circ \ , \\
\theta_{13}^\Lambda &= \frac{\theta_c}{3\sqrt{2}} + \mathcal{O}(\theta_c^3) \approx 3.1^\circ \ .
\end{aligned} \tag{29}$$

IV. HIGH SCALE STRUCTURE AND DOWNWARD EVOLUTION

As explained in the Introduction, our idea is to start with a specific structure of the neutrino mass matrix $\mathcal{M}_\nu^\Lambda$ that is dictated by some symmetry at a high scale $\Lambda \sim 10^{12}$ GeV. We would then like to evolve the elements of $\mathcal{M}_\nu$ down to a laboratory energy scale $\lambda \sim 10^3$ GeV. This involves studying the (one-loop) RG evolution of the coefficient functions $c_{\alpha\beta}$ in (18) between $\Lambda \sim 10^{12}$ GeV and $\lambda \sim 10^3$ GeV. In case the considered high scale neutrino symmetries are consequences of grand unification, we need to assume that the threshold effects [30] between the GUT scale $\sim 2 \times 10^{16}$ GeV and Λ are flavor blind so that they do not spoil the assumed symmetry relations in the downward evolution from $M_{\rm GUT}$ to Λ. We also note that effects of evolution on the masses and mixing angles of charged fermions are known [31] to be negligibly small [4] on account of the hierarchical nature of their mass values.

At one loop, the neutrino mass matrices at the scales Λ and λ are homogeneously related [32, 33]:

$$\mathcal{M}_\nu^\lambda = I_K \mathcal{I}_\kappa^T \ \mathcal{M}_\nu^\Lambda \ \mathcal{I}_\kappa \ , \tag{30}$$

where

$$I_K \equiv \exp\left[-\int_{t(\Lambda)}^{t(\lambda)} K(t) dt\right] \tag{31}$$

is a scalar factor common to all elements of $\mathcal{M}_\nu^\lambda$. In eq. (31), $t(Q) \equiv (16\pi^2)^{-1} \ln(Q/Q_0)$ with Q (Q_0) being a running (fixed) scale, and the integrand is given by

$$K(t) = -6g_2^2(t) - 2g_Y^2(t) + 6\mathrm{Tr}\ (Y_u^\dagger Y_u)(t) \tag{32}$$

[4] The value of $|V_{cb}|$ does run by about 0.01 in the MSSM due to the top quark U(1) coupling. However, at the level of accuracy that we are concerned with, this is inconsequential.

in a transparent notation, $g_{2,Y}$ being the $SU(2)_L, U(1)_Y$ gauge coupling strength and Y_u the up-type Yukawa coupling matrix. Finally, the matrix I_κ has the form

$$\mathcal{I}_\kappa \equiv \exp\left[-\int_{t(\Lambda)}^{t(\lambda)} (Y_l^\dagger Y_l)(t)dt\right] , \tag{33}$$

Y_ℓ being the Yukawa coupling matrix for charged leptons.

Although some of the neutrino mixing matrices in various scenarios in Sec. III have been motivated in terms of grand unification in bases where the symmetries involved may be clearly observed, for the RG evolution of all scenarios we choose to work in the basis where the charged lepton mass matrix is diagonal. In this basis,

$$Y_\ell^\dagger Y_\ell = \text{Diag}\ (y_e^2, y_\mu^2, y_\tau^2) . \tag{34}$$

We can neglect $y_{e,\mu}^2$ in comparison with y_τ^2 in (34) to get the result

$$\mathcal{I}_\kappa \approx\ \text{Diag}(1, 1, e^{-\Delta_\tau}) = \text{Diag}(1, 1, 1-\Delta_\tau) + \mathcal{O}(\Delta_\tau^2) , \tag{35}$$

where [32]

$$\Delta_\tau = \int_{t(\Lambda)}^{t(\lambda)} |y_\tau(t)|^2 = m_\tau^2(\tan^2\beta + 1)(8\pi^2 v^2)^{-1} \ln(\Lambda/\lambda) . \tag{36}$$

Here $v \equiv \sqrt{v_u^2 + v_d^2}$ and $\tan\beta = v_u/v_d$, where v_u (v_d) is $\sqrt{2}$ times the vev of the up (down) type neutral Higgs scalars. Evidently, Δ_τ is a small number for the allowed range of $\tan\beta$: e.g. $\Delta_\tau \approx 6 \times 10^{-3}$ for $\tan\beta = 30$, justifying our neglect of the $\mathcal{O}(\Delta_\tau^2)$ terms [5].

The substitution of (35) into (30) leads us to

$$\mathcal{M}_\nu^\lambda \propto \begin{pmatrix} 1 & 0 & 0 \\ 0 & 1 & 0 \\ 0 & 0 & 1-\Delta_\tau \end{pmatrix} \mathcal{M}_\nu^\Lambda \begin{pmatrix} 1 & 0 & 0 \\ 0 & 1 & 0 \\ 0 & 0 & 1-\Delta_\tau \end{pmatrix} + \mathcal{O}(\Delta_\tau^2) , \tag{37}$$

where the proportionality is through the scalar factor I_K given in (31). It must be emphasised that (37) is valid only when $\mathcal{M}_\nu^{\Lambda\,(\lambda)}$ is written in the basis where the charged lepton mass matrix is diagonal.

The matrix $\mathcal{M}_\nu^\Lambda$ is complex symmetric. Writing it in the general form

$$\mathcal{M}_\nu^\Lambda = \begin{pmatrix} A & B & C \\ B & D & E \\ C & E & F \end{pmatrix} , \tag{38}$$

[5] Note that a mistake of a factor of 2 in eq. 9 of [6] has been corrected here.

we have

$$\mathcal{M}_\nu^\lambda = \begin{pmatrix} A & B & C(1-\Delta_\tau) \\ B & D & E(1-\Delta_\tau) \\ C(1-\Delta_\tau) & E(1-\Delta_\tau) & F(1-2\Delta_\tau) \end{pmatrix} + \mathcal{O}(\Delta_\tau^2) \; . \tag{39}$$

Since both $M_\nu^{\Lambda,\lambda}$ are complex symmetric matrices, they can be diagonalized as

$$\begin{aligned} (U^\Lambda)^\dagger \; M_\nu^\Lambda (U^\Lambda)^* \; &= \; \mathrm{Diag}(|m_1^\Lambda|, |m_2^\Lambda|, |m_3^\Lambda|) \; , \\ (U^\lambda)^\dagger \; M_\nu^\lambda (U^\lambda)^* \; &= \; \mathrm{Diag}(|m_1^\lambda|, |m_2^\lambda|, |m_3^\lambda|) \; . \end{aligned} \tag{40}$$

Note that, since we are working in a basis where the charged lepton mass matrix is diagonal, $U^{\Lambda\ (\lambda)}$ is the same as the net leptonic mixing matrix $U_{\rm PMNS}$ (9) at the scale Λ (λ).

The unitary matrix $U_{\rm PMNS}$ may be parametrised in its most general form as

$$\begin{aligned} U_{\rm PMNS} \; \equiv \; & \mathrm{Diag}(e^{i\phi_e}, e^{i\phi_\mu}, e^{i\phi_\tau}) R_{23}(\theta_{23}) \mathrm{Diag}(1, 1, e^{i\delta_\ell}) R_{13}(\theta_{13}) \times \\ & \mathrm{Diag}(1, 1, e^{-i\delta_\ell}) R_{12}(\theta_{12}) \mathrm{Diag}(1, e^{-i\alpha_2/2}, e^{-i\alpha_3/2}) \, , \end{aligned} \tag{41}$$

where $R_{ij}(\theta_{ij})$ is the matrix for rotation through the angle θ_{ij} in the $i-j$ plane, δ_ℓ is the CP violating Dirac phase, $\alpha_{2,3}$ the Majorana phases and $\phi_{e,\mu,\tau}$ the so-called "unphysical" additional phases required to diagonalise the neutrino mass matrix. Here we have already used the freedom of choosing $\alpha_1 = 0$.

If θ_{13}^Λ vanishes on account of the symmetry requirement at the scale Λ, the evolution of the mixing angles can be computed analytically in a simple manner. The matrix U^Λ can then be written as

$$U^\Lambda = R_{23}(\theta_{23}^\Lambda) R_{12}(\theta_{12}^\Lambda) \mathrm{Diag}(1, e^{-i\alpha_2^\Lambda/2}, e^{-i\alpha_3^\Lambda/2}) \; , \tag{42}$$

since the Dirac phase contribution vanishes and the phases $\phi_{e,\mu,\tau}$ can anyway be absorbed in the charged lepton phases. RG evolution will modify the angles θ_{23}, θ_{12} as well as the phases $\alpha_{2,3}$, at the same time generating nonzero values for the mixing angle θ_{13} and the Dirac phase δ_ℓ. The phases $\phi_{e,\mu,\tau}$ that may get generated can always be absorbed in the phases of the charged lepton flavour eigenstates.

If we now approximate the deviation of U_ν^λ from U_ν^Λ by the retention of only terms that are linear in Δ_τ, we can write the modified mixing angles as

$$\theta_{12}^\lambda = \theta_{12}^\Lambda + k_{12}\Delta_\tau + \mathcal{O}(\Delta_\tau^2) \; , \; \theta_{23}^\lambda = \theta_{23}^\Lambda + k_{23}\Delta_\tau + \mathcal{O}(\Delta_\tau^2) \; , \; \theta_{13}^\lambda = k_{13}\Delta_\tau + \mathcal{O}(\Delta_\tau^2) \; . \tag{43}$$

The modified phases may similarly be written as

$$\alpha^{\lambda}_{2,3} = \alpha^{\Lambda}_{2,3} + a_{2,3}\Delta_\tau + \mathcal{O}(\Delta^2_\tau)\ ,\ \delta^{\lambda}_{\ell} = d_\ell \Delta_\tau + \mathcal{O}(\Delta^2_\tau)\ , \tag{44}$$

where we expect $a_{2,3}$ and d_ℓ to be $\mathcal{O}(1)$ quantities. In this paper we shall only be concerned about the deviation $k_{ij}\Delta_\tau$ of the mixing angles θ_{ij} from their high scale values. We shall see a posteriori that $|k_{ij}\Delta_\tau|$ is always much less than unity so that we can ignore its quadratic and higher powers.

The values of k_{ij} are found to be

$$\begin{aligned}
k_{12} &= \frac{1}{2}\sin 2\theta^{\Lambda}_{12}\sin^2\theta^{\Lambda}_{23}\frac{|m^{\Lambda}_1 + m^{\Lambda}_2|^2}{|m^{\Lambda}_2|^2 - |m^{\Lambda}_1|^2}\ , \\
k_{23} &= \frac{1}{2}\sin 2\theta^{\Lambda}_{23}\left(\cos^2\theta^{\Lambda}_{12}\frac{|m^{\Lambda}_2 + m^{\Lambda}_3|^2}{|m^{\Lambda}_3|^2 - |m^{\Lambda}_2|^2} + \sin^2\theta^{\Lambda}_{12}\frac{|m^{\Lambda}_1 + m^{\Lambda}_3|^2}{|m^{\Lambda}_3|^2 - |m^{\Lambda}_1|^2}\right)\ , \\
k_{13} &= \frac{1}{4}\sin 2\theta^{\Lambda}_{12}\sin 2\theta^{\Lambda}_{23}\left(\frac{|m^{\Lambda}_2 + m^{\Lambda}_3|^2}{|m^{\Lambda}_3|^2 - |m^{\Lambda}_2|^2} - \frac{|m^{\Lambda}_1 + m^{\Lambda}_3|^2}{|m^{\Lambda}_3|^2 - |m^{\Lambda}_1|^2}\right)\ ,
\end{aligned} \tag{45}$$

where m^{Λ}_i are the masses $|m^{\Lambda}_i|e^{i\alpha^{\Lambda}_i}$ at the high scale. The RG evolution of $|m_i|$ may be parametrised by

$$|m^{\lambda}_i| = I_K |m^{\Lambda}_i|\left(1 + \mu_i\Delta_\tau + \mathcal{O}(\Delta^2_\tau)\right) \tag{46}$$

where I_K is the scalar factor given in (31) and μ_i are $\mathcal{O}(1)$ numbers [24]. Then, taking m_i to be the masses $|m^{\lambda}_i|e^{i\alpha^{\lambda}_i}$ at the low scale introduces an error of $\mathcal{O}(\Delta_\tau)$ in k_{ij}, and hence of $\mathcal{O}(\Delta^2_\tau)$ in θ_{ij}. Eqs. (45) are therefore valid even with the low scale values of the masses and Majorana phases. The same argument is true even for the mixing angles θ_{ij}. Since all observations in the neutrino experiments are made at laboratory energies, we henceforth drop the superscript λ for all the quantities at the low scale.

The expressions (45) have been derived starting with $\theta^{\Lambda}_{13} = 0$, and they agree with the general expressions in [24] in the limit $\theta^{\Lambda}_{13} \to 0$. For finite θ^{Λ}_{13}, the k_{ij} given in (45) have an error of $\mathcal{O}(\theta^{\Lambda}_{13})$, i.e. the mixing angles at the low scale have an error of $\mathcal{O}(\theta^{\Lambda}_{13}\Delta_\tau)$, which we neglect in our analytical approximations. Since for all the scenarios considered here, $\theta^{\Lambda}_{13}\Delta_\tau \lesssim 0.1^\circ$, this is a justified assumption. Thus, even with small nonzero values of θ^{Λ}_{13}, as is the case with QLC1, QLC2 and TBM2 scenarios, we can justifiably use the result $\theta_{ij} \approx \theta^{\Lambda}_{ij} + k_{ij}\Delta_\tau$ with k_{ij} given by (45). Another requirement for the validity of eqs. (45) is that the values of m_i and $|m_i|^2 - |m_j|^2$ should be described accurately by the $\mathcal{O}(\Delta_\tau)$ terms in their RG evolution. This condition does not impose any restriction on m^{Λ}_i. However,

for $\Delta_\tau \gtrsim (|m_2^\Lambda|^2 - |m_1^\Lambda|^2)/(m_0^\Lambda)^2$, the $\mathcal{O}(\Delta_\tau^2)$ terms dominate over the $\mathcal{O}(\Delta_\tau)$ terms in the $|m_2|^2 - |m_1|^2$ evolution [24], which results in eqs. (45) breaking down. Thus for the validity of these equations, we require

$$(m_0^\Lambda)^2 \cdot \Delta_\tau \lesssim |m_2^\Lambda|^2 - |m_1^\Lambda|^2 \; . \tag{47}$$

Eq. (47) may be violated if $|m_2^\Lambda|^2 - |m_1^\Lambda|^2$ is indeed very small. However, even in such a situation, many of the qualitative features following from our analytical treatment will continue to remain valid. This will be confirmed by the exact numerical analysis given later.

One can make some further observations on eqs. (45). Since k_{12} is always positive, the measured value of θ_{12} can never be smaller than θ_{12}^Λ. Moreover, in order to have any significant effect of RG evolution, some $|k_{ij}|$ are required to be $\gtrsim \mathcal{O}(10)$ since $\Delta_\tau \lesssim \mathcal{O}(10^{-2})$. This requirement is not met in the case of a normal hierarchy which has all $|k_{ij}| \sim \mathcal{O}(1)$, and hence there is no significant RG effect there. Specifically, for an enhancement of $|k_{12}|$, $|m_0^\Lambda|^2$ must necessarily be $\gg |m_2^\Lambda|^2 - |m_1^\Lambda|^2$. This inequality is obeyed whenever neutrinos are nonhierarchical, i.e. either in the IH or the QD case. On the other hand, the enhancement of both $|k_{23}|$ and $|k_{13}|$ requires the inequality $|\rho_A^\Lambda| \ll 1$, satisfied only by QD neutrinos. However, these are necessary conditions. The occurence (or not) of an actual enhancement depends on the Majorana phases $\alpha_{2,3}$ too. In order to see this dependence explicitly, let us rewrite (45) in terms of these phases and our parameters ρ_A^Λ and ϵ_S^Λ of (12), defined at the high scale. We then have, with finite θ_{13}^Λ,

$$\begin{aligned}
k_{12} &= \frac{1}{4\epsilon_S^\Lambda} \sin 2\theta_{12}^\Lambda \sin^2\theta_{23}^\Lambda \left[1 + \cos\alpha_2^\Lambda + (\epsilon_S^\Lambda)^2(1 - \cos\alpha_2^\Lambda)\right] + \mathcal{O}(\theta_{13}^\Lambda) \; , \\
k_{23} &= \frac{\Gamma^\Lambda}{4} \sin 2\theta_{23}^\Lambda \left[1 + \cos^2\theta_{12}^\Lambda \cos(\alpha_2^\Lambda - \alpha_3^\Lambda) + \sin^2\theta_{12}^\Lambda \cos\alpha_3^\Lambda\right] \\
&\qquad + \frac{\rho_A^\Lambda}{2} \sin 2\theta_{12}^\Lambda \sin 2\theta_{23}^\Lambda + \mathcal{O}(\epsilon_S^\Lambda, \theta_{13}^\Lambda) \; , \\
k_{13} &= \frac{\Gamma^\Lambda}{8} \sin 2\theta_{12}^\Lambda \sin 2\theta_{23}^\Lambda \left[\cos(\alpha_2^\Lambda - \alpha_3^\Lambda) - \cos\alpha_3^\Lambda\right] + \mathcal{O}(\epsilon_S^\Lambda, \theta_{13}^\Lambda) \; .
\end{aligned} \tag{48}$$

It is clear from (48) that the values of the Majorana phases $\alpha_{2,3}^\Lambda$ are crucial in controlling whether the evolution terms $k_{ij}\Delta_\tau$ are dangerously large or not. For instance, as $\alpha_2^\Lambda \to 0$, we have $k_{12} \approx (4\epsilon_S^\Lambda)^{-1}$. For nonhierarchical neutrinos, the latter is likely to destroy any high scale symmetry statement on θ_{12}. When α_2^Λ increases from zero, $|k_{12}|$ decreases rapidly, becoming as small as $|\epsilon_S^\Lambda|/4$ when $\alpha_2^\Lambda = \pi$, i.e. $m_1^\Lambda \approx -m_2^\Lambda$. Moreover, (48) also indicates

that both $|k_{23}|$ and $|k_{13}|$ are enhanced when either $\alpha_3^\Lambda = 0$, or $\alpha_2^\Lambda = \alpha_3^\Lambda$ for a nonzero α_2^Λ, though $|k_{13}|$ gets highly suppressed when $\alpha_2^\Lambda = 0$.

As noted in Sec. II, the sign of Γ^Λ is positive for a normal ordering and negative for an inverted ordering of the neutrino masses. Thus k_{23} is always positive (negative) for a normal (inverted) ordering. However, the sign of k_{13} is controlled not only by $\mathrm{sgn}(\Gamma^\Lambda)$ but also by a combination of Majorana phases.

In the remaining part of this section, we enumerate the predictions for the four scenarios considered in this paper. On evolution down to the scale λ, the mixing angles of the corresponding mixing matrix $U_{\rm PMNS}$ are given in all the four cases by $\theta_{ij} = \theta_{ij}^\Lambda + k_{ij}\Delta_\tau + \mathcal{O}(\theta_{13}^\Lambda\Delta_\tau, \Delta_\tau^2)$ where the values of k_{ij} are given by (48).

A. QLC1

On evolving (22) to the laboratory scale, the net leptonic mixing angles are found to be

$$\begin{aligned}
\theta_{12} &= \frac{\pi}{4} - \frac{\theta_c}{\sqrt{2}} + k_{12}^{\rm QLC1}\Delta_\tau + \mathcal{O}(\theta_c^3, \theta_{13}^\Lambda\Delta_\tau, \Delta_\tau^2)\,, \\
\theta_{23} &= \frac{\pi}{4} - |V_{cb}| - \frac{\theta_c^2}{4} + k_{23}^{\rm QLC1}\Delta_\tau + \mathcal{O}(\theta_c^3, \theta_{13}^\Lambda\Delta_\tau, \Delta_\tau^2)\,, \\
\theta_{13} &= \left|\frac{\theta_c}{\sqrt{2}} - k_{13}^{\rm QLC1}\Delta_\tau\right| + \mathcal{O}(\theta_c^3, \theta_{13}^\Lambda\Delta_\tau, \Delta_\tau^2)\,,
\end{aligned} \tag{49}$$

where the neglected terms are $\lesssim 0.1^\circ$. The absolute value taken for the RHS of θ_{13} is in order to keep to the convention of defining $\theta_{ij} > 0$ [28].

Since $\pi/4 - \theta_c/\sqrt{2} \approx 35.4^\circ$ and $k_{12}^{\rm QLC1}\Delta_\tau > 0$, it follows from (49) that θ_{12} in this scenario cannot be less than 35.4°. Further, since $\pi/4 - |V_{cb}| - \theta_c^2/4 \approx 42.1^\circ$, and $k_{23}^{\rm QLC1}\Delta_\tau > 0$ (< 0) for a normal (inverted) ordering of neutrino masses, a consequence of (49) is that θ_{23} is greater than (less than) 42.1° for a normal (inverted) ordering. Finally, the predicted value of θ_{13} is $\theta_c/\sqrt{2} \approx 8.9^\circ$ in the absence of RG running, but it can be greater or less than 8.9° depending on the values of the Majorana phases. The detailed numerical analysis will be presented in Sec. V.

B. QLC2

After RG evolution, the high scale angles (25) in this scenario evolve to

$$\begin{aligned}
\theta_{12} &= \frac{\pi}{4} - \theta_c + k_{12}^{\rm QLC2}\Delta_\tau - + \mathcal{O}(\theta_c^3, \theta_{13}^\Lambda\Delta_\tau, \Delta_\tau^2) \ , \\
\theta_{23} &= \frac{\pi}{4} - \frac{|V_{cb}|}{\sqrt{2}} + k_{23}^{\rm QLC2}\Delta_\tau + \mathcal{O}(\theta_c^3, \theta_{13}^\Lambda\Delta_\tau, \Delta_\tau^2) \ , \\
\theta_{13} &= \left| \frac{|V_{cb}|}{\sqrt{2}} - k_{13}^{\rm QLC2}\Delta_\tau \right| + \mathcal{O}(\theta_c^3, \theta_{13}^\Lambda\Delta_\tau, \Delta_\tau^2) \ ,
\end{aligned} \tag{50}$$

where the neglected terms are $\lesssim 0.1^\circ$ as before.

The lower bound on θ_{12} in this scanario being $\pi/4 - \theta_c \approx 32.4^\circ$, significantly lower values of θ_{12} than QLC1 are allowed. Also, here θ_{23} is greater than (less than) $\pi/4 - |V_{cb}|/\sqrt{2} \approx 43.4^\circ$ for normal (inverted) neutrino mass ordering. The major difference from QLC1 is in θ_{13}: the value θ_{13} in QLC2 is only $|V_{cb}|/\sqrt{2} \approx 1.6^\circ$ in the absence of RG running. It can increase with RG running, but the extent of this increase is restricted from the observed θ_{12} values which restrict the values of the Majorana phases in turn. The detailed numerical analysis will again be presented in Sec. V.

C. TBM1

The mixing angles at the low scale here are simply given by

$$\begin{aligned}
\theta_{12} &= \sin^{-1}\frac{1}{\sqrt{3}} + k_{12}^{\rm TBM1}\Delta_\tau + \mathcal{O}(\theta_c^3, \theta_{13}^\Lambda\Delta_\tau, \Delta_\tau^2) \ , \\
\theta_{23} &= \frac{\pi}{4} + k_{23}^{\rm TBM1}\Delta_\tau + \mathcal{O}(\theta_c^3, \theta_{13}^\Lambda\Delta_\tau, \Delta_\tau^2) \ , \\
\theta_{13} &= k_{13}^{\rm TBM1}\Delta_\tau + \mathcal{O}(\theta_c^3, \theta_{13}^\Lambda\Delta_\tau, \Delta_\tau^2) \ .
\end{aligned} \tag{51}$$

On similar lines to the arguments given for the QLC scenarios, here (i) the minimum value of θ_{12} is $\sin^{-1}(1/\sqrt{3}) \approx 35.3^\circ$, (ii) the value of θ_{23} is greater than (less than) 45° for normal (inverted) hierarchy, and the value of θ_{13} vanishes in the absence of RG running. Since (48) shows that θ_{13} does not run if the Majorana phases vanish, *any observed deviation of θ_{13} from zero in this scheme will indicate nonvanishing Majorana phases.* The detailed numerical analysis appears in Sec. V.

D. TBM2

The mixing angles (29) for this scenario evolve to the laboratory scale and become

$$\begin{aligned}
\theta_{12} &= \sin^{-1}\frac{1}{\sqrt{3}} - \frac{\theta_c}{3\sqrt{2}} + k_{12}^{\rm TBM2}\Delta_\tau + \mathcal{O}(\theta_c^3, \theta_{13}^\Lambda\Delta_\tau, \Delta_\tau^2) \,, \\
\theta_{23} &= \frac{\pi}{4} - |V_{cb}| + k_{23}^{\rm TBM2}\Delta_\tau + \mathcal{O}(\theta_c^3, \theta_{13}^\Lambda\Delta_\tau, \Delta_\tau^2) \,, \\
\theta_{13} &= \left|\frac{\theta_c}{3\sqrt{2}} - k_{13}^{\rm TBM2}\Delta_\tau\right| + \mathcal{O}(\theta_c^3, \theta_{13}^\Lambda\Delta_\tau, \Delta_\tau^2) \,. \qquad (52)
\end{aligned}$$

The minimum allowed value of θ_{12} in this scenario is $\sin^{-1}(1/\sqrt{3}) - \theta_c/(3\sqrt{2}) \approx 32.3^\circ$, since $k_{12}^{\rm TBM2} > 0$. The value of θ_{23} is greater than (less than) $\pi/4 - |V_{cb}| \approx 42.7^\circ$ for normal (inverted) hierarchy. Finally, the value of θ_{13} is $\theta_c/(3\sqrt{2}) \approx 3.1^\circ$ in the absence of RG running. Again, the detailed numerical analysis with RG running is presented in Sec. V.

V. CONSTRAINTS ON m_0, $\tan\beta$ AND MAJORANA PHASES

In this section, we explore the current limits on the parameters of the four scenarios considered above. The main parameters governing RG running are m_0, $\tan\beta$, the Majorana phases $\alpha_{2,3}$, and (to a smaller extent) the Dirac phase δ_ℓ. Our aim is to find the range of values of these parameters allowed by the current data. The four scenarios also lead to slightly different predictions for the mixing angles; and accurate measurements of these angles should distinguish among them in the absence of RG running. However, since the latter spoils high scale symmetries in general, and since the values of all the relevant parameters are still not known, the low scale predictions of the mixing angles are expected to ovelap. We explore in detail whether this still allows one to discriminate among the scenarios considered in this paper. Moreover, we study the correlations between the deviations of the mixing angles from their high scale values.

We use the 3σ ranges for the neutrino mass and mixing parameters

$$7\times10^{-5}\ {\rm eV}^2 < \delta m_S^2 < 9.1\times10^{-5}\ {\rm eV}^2 \,, \quad 1.7\times10^{-3}\ {\rm eV}^2 < |\delta m_A^2| < 3.3\times10^{-3}\ {\rm eV}^2 \,, \qquad (53)$$

$$30^\circ < \theta_{12} < 39.2^\circ \,, \quad 35.5^\circ < \theta_{23} < 55.5^\circ \,, \qquad \theta_{13} < 12^\circ \qquad (54)$$

at the low scale. At the high scale, we start with the values of θ_{ij}^Λ dictated by the scenario under consideration, and a range of $\delta m_{S/A}^2$ values that are consistent, after RG evolution,

with the low scale measurements (53) and (54). We show our results for a normal mass ordering of neutrinos. However, the constraints in the case of an inverted mass ordering are almost identical.

We give our constraints in terms of the values of m_0^Λ and α_2^Λ at the high scale. These are related to the low scale values of m_0 and α_2 as indicated in (46) and (44) respectively. In particular, the evolution of m_0 is controlled mainly by $I_K \approx 0.71$, which makes $m_0^\lambda \approx 0.71\, m_0^\Lambda$. The bounds on m_0^Λ shown in the figures in this section can then be easily translated into bounds on the low scale value of m_0. The RG evolution of α_2 is given by $\alpha_2^\lambda \approx \alpha_2^\Lambda + a_2 \Delta_\tau$ with [24]

$$a_2 \approx \frac{-4|m_1^\Lambda m_2^\Lambda|}{|m_2^\Lambda|^2 - |m_1^\Lambda|^2} \cos 2\theta_{12}^\Lambda \sin^2 \theta_{23}^\Lambda \sin \alpha_2^\Lambda \ , \tag{55}$$

which may be used to translate the α_2^Λ constraints to low scale values of α_2.

We have neglected possible Planck scale effects [37] which may change the value of θ_{12} by a few degrees for quasidegenerate neutrinos, leaving the other two angles virtually unaffected. Inclusion of these effects would relax [38] the constraints in the m_0^Λ – α_2^Λ plane by a small amount.

A. Limits on m_0^Λ, α_2^Λ and $\tan\beta$

Out of the three leptonic mixing angles, θ_{12} is the one measured with the greatest accuracy currently. Since all the scenarios have specific predictions for θ_{12} in the absence of RG evolution, the measured value of θ_{12} can put the strongest constraints on the running parameters. From (43) and (48), the running of θ_{12} is expected to be independent of α_3^Λ.

We show in Fig. 2 the 3σ allowed regions in the $m_0^\Lambda - \alpha_2^\Lambda$ plane for two $\tan\beta$ values. This figure has been obtained from numerical solutions of the RG equations. The figure agrees very well with our expectations from the analytic expressions (48). On account of the occurence of the small quantity ϵ_S in the denominator of k_{12} in eq. (48), strong constraints ensue on m_0^Λ and α_2^Λ. At large $\tan\beta$ (equivalent to a relatively large Δ_τ), the value of α_2^Λ has to be near π (i.e. $m_1^\Lambda \approx -m_2^\Lambda$) underscoring the necessity for a nontrivial Majorana phase. However, the requirement is less severe for a smaller $\tan\beta$. The coefficient a_2 in (55) characterising the evolution of α_2 vanishes when $\alpha_2^\Lambda = \pi$ [24]. As a result, the preferred value of α_2, viz. $\alpha_2^\Lambda = \pi$, is equivalent to $\alpha_2 = \pi$ at all scales.

The constraints displayed in the figure are calculated for two fixed $\tan\beta$ values. The

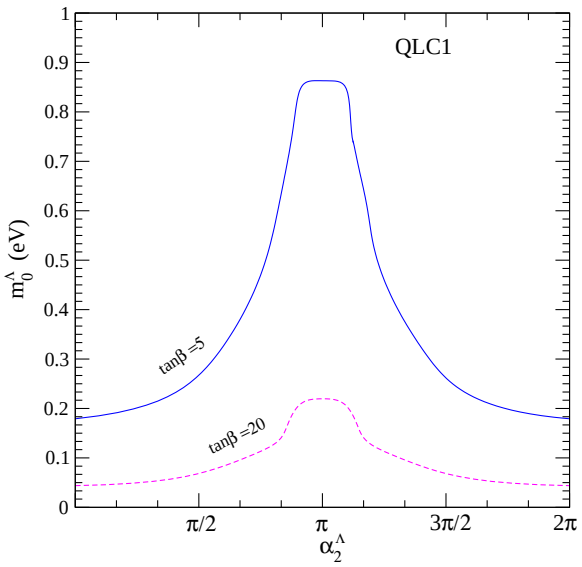

FIG. 2: Constraints from the 3σ allowed range of θ_{12} on the m_0 (eV) – α_2 (radians) parameter space for $\tan\beta = 5$ and 20 in the QLC1 scenario. The regions above the contours are excluded by data for that particular value of $\tan\beta$. The peak at $\alpha_2 \approx \pi$ is noteworthy.

results for other values of $\tan\beta$ may be extrapolated from the figure. However, we observe numerically that the θ_{12} constraints on the m_0^Λ – α_2^Λ plane (Fig. 2) depend essentially on the combination $m_0^\Lambda \tan\beta$. Therefore, in Fig. 3, we show the allowed region in the $m_0 \tan\beta$ – α_2 parameter space for all four scenarios. The differences among the four scenarios arise primarily from the differences in the values of θ_{12}^Λ. These are 35.4° (QLC1), 32.4° (QLC2), 35.3° (TBM1) and 32.3° (TBM2) in the four scenarios. The deviation of θ_{12} from this value, $\Delta\theta_{12} \equiv \theta_{12} - \theta_{12}^\Lambda$ differs in all the scenarios only through a factor of $\sin 2\theta_{12}^\Lambda \sin^2\theta_{23}^\Lambda$ [see eq. (48)], which is equal to unity within 5% for all the four scenarios. As a result, the allowed regions for QLC2 and TBM2 are nearly identical, and larger than those for QLC1 and TBM1, the last two regions being also almost identical to each other.

Note that, for all the scenarios, the larger the value of $m_0^\Lambda \tan\beta$, the closer the value of α_2^Λ needs to be to π. This statement is true even if we use the laboratory values of m_0 and α_2. Moreover, the region with $m_0^\Lambda \tan\beta \gtrsim 4.4$ eV (i.e. $m_0 \tan\beta \gtrsim 3.1$ eV) is disallowed for all values of α_2 and for all scenarios.

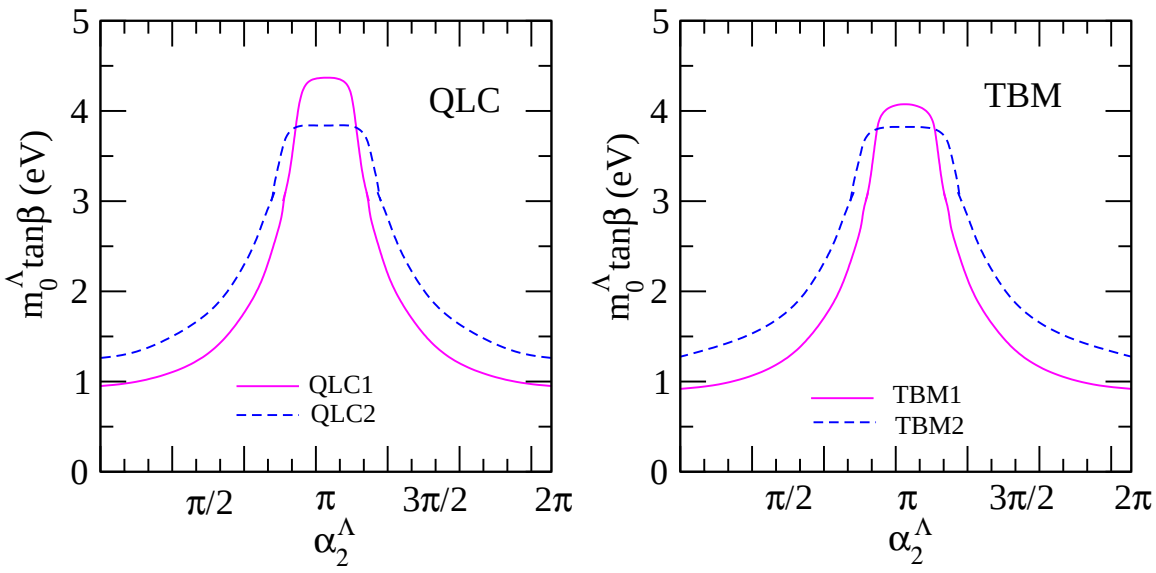

FIG. 3: Constraints from the 3σ allowed range of θ_{12} on the $m_0 \tan\beta$ (eV) – α_2 (radians) parameter space for the four scenarios. The regions above the contours are excluded by data for that particular scenario.

B. θ_{13} to discriminate among scenarios

The four scenarios that we consider here give different predictions for the values of θ_{13}^Λ: 8.9° (QLC1), 1.6° (QLC2), 0° (TBM1) and 3.1° (TBM2). In the absence of RG running, therefore, a discrimination between some of these scenarios should be possible in the near future. For example, if QLC1 is realised in nature, the value of θ_{13} would be accessible to the current generation of experiments. However, the value of θ_{13} changes with RG evolution and can either increase or decrease depending on the values of Majorana phases, as can be seen from (48). It is conceivable that the allowed ranges of θ_{13} values for all the scenarios will then overlap and the power of discrimination will be lost. It is thus worthwhile to check whether one retains this discrimination capability in spite of the RG running. What helps in this is the fact that at higher values of $m_0^\Lambda \tan\beta$, where one expects large RG effects, not all $\alpha_{2,3}^\Lambda$ values are allowed: the observed values of θ_{12} (as shown in Sec. V A) as well as of θ_{23} restrict the values of the Majorana phases, which in turn restrict the allowed values of θ_{13}.

In Fig. 4, we show the pemitted values of θ_{13} in the four scenarios, subject to the constraints of the 3σ allowed current ranges of the mixing angles. With the current constraints, it should be possible to distinguish between QLC1 and the other scenarios in the next round

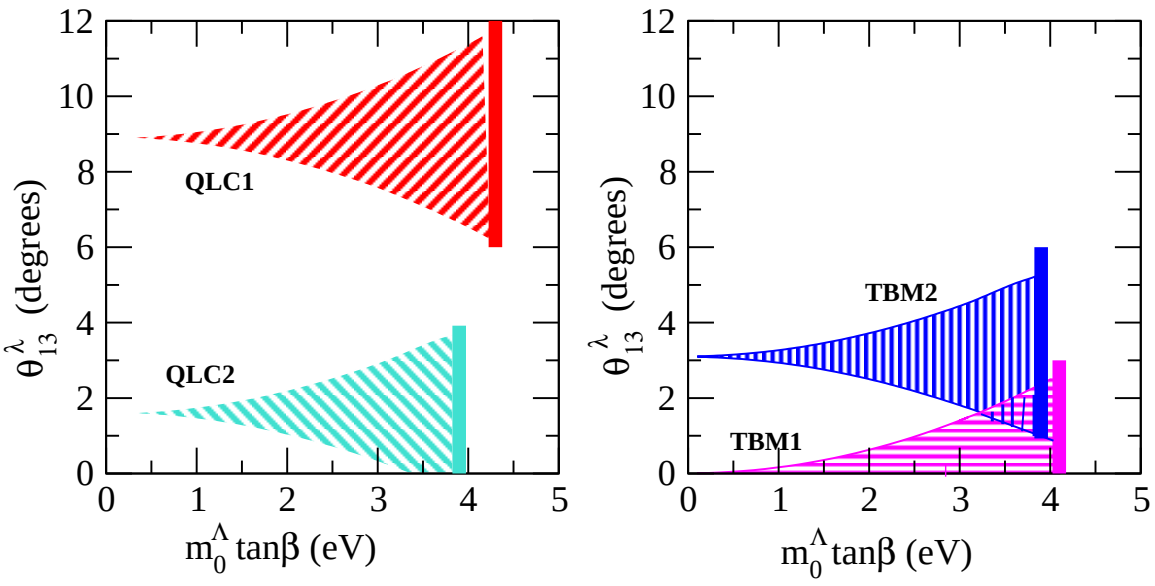

FIG. 4: Values of θ_{13} in the QLC scenarios (left panel) and the TBM scenarios (right panel) as a function of $m_0 \tan\beta$, allowed with the current constraints on the mixing angles and mass squared differences. The shaded region represents the allowed values of θ_{13} at the laboratory scale in each scenario. The thick bands represent upper limits on $m_0^{\Lambda} \tan\beta$ from current measurements.

of experiments [39] probing θ_{13}. For example, if θ_{13} is shown to be less than 6°, QLC1 will be excluded.

The scenario TBM2 may be distinguishable from the remaining two cases if $m_0^{\Lambda} \tan\beta \lesssim 2$ eV (i.e. $m_0 \tan\beta \lesssim 1.4$ eV). So this needs, in addition to the information on θ_{13}, stronger constraints on the values of m_0 or $\tan\beta$. A more accurate measurement [40] of θ_{12} will also indirectly limit the extent of RG evolution and may enable one to distinguish TBM2 from the other two scenarios, viz. QLC2 and TBM1. The last two scenarios have very similar predictions on θ_{13}. This is on account of the close values of θ_{13}^{Λ} in the two scenarios, and the nearly identical evolution $\Delta\theta_{13} \equiv \theta_{13} - \theta_{13}^{\Lambda}$ in them, whatever the values of $\alpha_2^{\Lambda}, \alpha_3^{\Lambda}, m_0^{\Lambda}$ and $\tan\beta$. From (48), the value of $\Delta\theta_{13}$ differs in all the scenarios only through a factor of $\sin 2\theta_{12}^{\Lambda} \sin 2\theta_{23}^{\Lambda}$ [see eq. (48)], which is equal to unity within 5% for all the four scenarios. Therefore, distinguishing between these two scenarios on the basis of a measurement of θ_{13} alone will be difficult unless the values of the other parameters – $m_0^{\Lambda}, \tan\beta, \alpha_2^{\Lambda}, \alpha_3^{\Lambda}$ – are also known to a good accuracy.

Though the constraints on $m_0^{\Lambda} \tan\beta$ and α_2^{Λ} in sec. V A are logarithmically sensitive to the choice of the high scale Λ, the limits on θ_{13} in a given scenario are almost indepenent of

Λ. This is because the maximum allowed value of $|\Delta\theta_{13}|$ is dictated mainly by the maximum allowed value of $\Delta\theta_{12}$ through $|\Delta\theta_{13}|/\Delta\theta_{12} \approx |k_{13}|/k_{12}$, whereas the maximum allowed value of $\Delta\theta_{12}$ in turn is an experimentally determined quantity, quite independent of Λ.

C. Effect of RG evolution on θ_{23}

The predictions of all the scenarios for θ_{23} are almost identical. The values of θ_{23}^{Λ} are very close: 42.1° (QLC1), 43.4° (QLC2), 45° (TBM1) and 42.7° (TBM2). Moreover, the deviations $\Delta\theta_{23} \equiv \theta_{23} - \theta_{23}^{\Lambda}$ are almost independent of the scenario, but depend on the value of α_3^{Λ}. This may be shown as follows: at large values of m_0^{Λ} that are needed to have significant RG running, at the high scale $|\rho_A^{\Lambda}| \ll 1$, so that $\Gamma^{\Lambda} \approx 1/\rho_A^{\Lambda}$, and the value of α_2^{Λ} is restricted to be very close to π. As a result, (48) gives

$$\Delta\theta_{23} \approx \frac{\Delta_\tau}{\rho_A^{\Lambda}} \sin 2\theta_{23}^{\Lambda}(1 - \cos 2\theta_{12}^{\Lambda} \cos\alpha_3^{\Lambda}) \tag{56}$$

which is almost independent of the scenario on account of similar values of θ_{23}^{Λ} and θ_{12}^{Λ}, but may vary by $\approx \cos 2\theta_{12}^{\Lambda} \approx 30\%$ depending on the value of α_3^{Λ}. As a consequence, a measurement of θ_{23} cannot discriminate between the four scenarios unless it is accurate to the level of a degree. However, if a scenario has already been identified, the measured value of θ_{23} will restrict the allowed values of the Majorana phase α_3^{Λ}.

VI. DISCUSSION AND SUMMARY

The current data on neutrino masses and mixings angles are consistent with symmetry-based schemes like quark-lepton complementarity (QLC) or tribimaximal mixing (TBM). These scenarios predict specific values of the neutrino mixing angles, which need to be compared with their forthcoming more accurately measured values in order to confirm or exclude a particular postulated symmetry pattern. However, the symmetry relations need to be imposed at a high scale, e.g. the seesaw scale $\sim 10^{12}$ GeV, where the neutrino masses originate. Radiative corrections to the neutrino masses in general do not respect the symmetries involved in QLC or TBM. As a result, predictions of the neutrino parameters measured at laboratory energies become different from those given by these symmetries at the high scale. It is therefore necessary to obtain low scale predictions of these scenarios.

We have calculated radiative corrections to the neutrino mixing angles θ_{ij} in the context of the minimal supersymmetric standard model (MSSM). We have taken the low scale to be the supersymmetry breaking scale $\sim 10^3$ GeV and have neglected threshold effects, if any, during this renormalisation group (RG) evolution. We have presented a technique to calculate the deviations $\Delta\theta_{ij}$ of the mixing angles from their high scale values. This technique yields analytically transparent results where the errors, caused by the approximations made, are small and under control. The analytic treatment clarifies the dependence of the RG running of neutrino mixing angles on currently unknown parameters like the mass scale m_0 of neutrinos, the value of $\tan\beta$ in MSSM and the values of the Majorana phases. We have also solved the RG equations numerically to confirm that the results are indeed closely approximated by our analytical expressions.

We have pointed out certain important patterns in the RG evolution of the mixing angles that are valid in any scenario. The RG running of θ_{12} always increases its value from the high to the low scale. Therefore, if a scenario predicts the value of θ_{12}^{Λ} at the high scale Λ, the low scale measurement must be $\theta_{12} > \theta_{12}^{\Lambda}$ in order for the scenario to stay valid. Similarly, the value of θ_{23} increases (decreases), while running from a high to a low scale, for a normal (inverted) neutrino mass ordering. The value of θ_{13} is controlled not only by mass ordering, but also by the values of the Majorana phases, depending on which it may increase or decrease with RG running.

We have considered two versions of the QLC principle (QLC1 and QLC2) and two versions of the TBM scheme (TBM1 and TBM2), whose predictions at the high scale are consistent with the measured neutrino mixing angles at laboratory energies. The PMNS mixing matrices at the high scale predicted within these scenarios are $V_{\rm CKM}^{\dagger}U_{\nu,\rm bm}$ (QLC1), $U_{\nu,\rm bm}V_{\rm CKM}^{\dagger}$ (QLC2), $U_{\nu\rm tbm}$ (TBM1) and $V_{\ell L}^{\dagger}U_{\nu,\rm tbm}$ (TBM2) respectively, where $V_{\rm CKM}$ is the CKM matrix, $U_{\nu,\rm bm}$ the bimaximal mixing matrix, $U_{\nu,\rm tbm}$ the tribimaximal [12] mixing matrix, and $V_{\ell L}$ a charged lepton mixing matrix inspired by the Georgi-Jarlskog relation [36] at the GUT scale.

We summarise our findings in three items:

(i) The RG running of the mixing angles should not be too large lest the low energy values differ too much from their high energy predictions. Since θ_{12} is the most accurately measured angle currently, that puts strong constraints on the allowed values of $m_0^{\Lambda}\tan\beta$ as well as on the Majorana phase α_2^{Λ}. It is observed that, for $m_0^{\Lambda}\tan\beta \gtrsim 2$ eV (i.e. $m_0\tan\beta \gtrsim 1.4$

eV), the allowed range of α_2^Λ is severely restricted. In all the scenarios, $m_0^\Lambda \tan\beta$ has to be $\lesssim 4.4$ eV (i.e. $m_0 \tan\beta$ has to be $\lesssim 3.1$ eV) for consistency with data. Moreover, the larger the value of $m_0 \tan\beta$, the closer to π has to be the value of α_2^Λ, and hence that of α_2 at the laboratory scale, cf. eq. (55). Thus we find a preference for the approximate equality $m_1 \simeq -m_2$ (especially for large $\tan\beta$), as also suggested by considerations of leptogenesis [21]. A reduction of errors on the θ_{12} measurement would decrease the allowed area in the $m_0^\Lambda \tan\beta - \alpha_2^\Lambda$ plane. Moreover, since θ_{12} always increases from higher to lower scales, if its value is measured to be smaller than what is predicted at the high scale in a scenario, that particular scenario would get excluded. *All the scenarios considered in this paper would be excluded if θ_{12} were measured to be less than 32°.*

(ii) The measurement of θ_{13} is most likely to serve as a discriminator among the four scenarios considered here. The predicted values of θ_{13} in these scenarios at the high scale are 8.9° (QLC1), 1.6° (QLC2), 0° (TBM1) and 3.1° (TBM2). RG running can modify the value of θ_{13} in either direction; however, the restrictions on $m_0^\Lambda \tan\beta$ and α_2^Λ from the θ_{12} measurements limit the extent of this modification. We find, for example, that the value of θ_{13} in QLC1 cannot be less than 6° (3σ), whereas in none of the other cases can θ_{13} be as large as 6° within 3σ. Neutrino experiments during the next decade should be able to measure the value of θ_{13} if it is greater than $\approx 5^\circ$ or to put an upper bound of $\approx 5^\circ$ on it. In either case, the scanario QLC1 will be distinguishable from the others. Both QLC2 and TBM1 predict almost identical θ_{13} ranges: $\theta_{13} < 3^\circ$ (3σ). The allowed 3σ range of θ_{13} for TBM2 overlaps with the QLC2/TBM1 range for $m_0^\Lambda \tan\beta \gtrsim 2$ eV (i.e. $m_0 \tan\beta \gtrsim 1.4$ eV). Limiting $m_0 \tan\beta$ to lesser values would also help in discriminating between TBM2 on one hand, and QLC1/TBM2 on the other.

(iii) It is not possible for a θ_{23} measurement to discriminate among the four scenarios unless it is accurate to the level of a degree. However the value of θ_{23} within any scenario is strongly dependent on the Majorana phase α_3^Λ. Therefore, if a scenario has already been identified, the measured value of θ_{23} will restrict the allowed values of α_3^Λ.

In conclusion, we have shown how the high scale predictions on neutrino mixing angles get modified with RG running in MSSM for four symmetry-inspired scenarios that are consistent with the current neutrino data. With a combination of analytical insights and numerical calculations, we show that this limits the allowed ranges of parameters like m_0^Λ, $\tan\beta$ and the Majorana phases. We also indicate the extent to which future measurements

can discriminate among various scenarios and how the values of the parameters may be further restricted.

Acknowledgements

A.D. and S.G. would like to thank W. Rodejohann for useful discussions. P.R. acknowledges the hospitality of the University of Hawaii at Manoa where part of this work was carried out. The work of A.D. is partly supported through the Partner Group program between the Max Planck Institute for Physics and Tata Institute of Fundamental Research. Part of the computational work for this study were carried out at cluster computing facility in the Harish-Chandra Research Institute (http://www.cluster.mri.ernet.in).

---

[1] R. N. Mohapatra *et al.*, arXiv:hep-ph/0510213; R. N. Mohapatra and A. Yu. Smirnov, Ann. Rev. Nucl. Part. Sci. **56**, 569 (2006).

[2] J. Schechter and J. W. F. Valle, Phys. Rev. D **22**, 2227 (1980).

[3] S. Antusch and S. F. King, Nucl. Phys. B **705**, 239 (2005); their Refs. [13-22]; G. C. Branco, M. N. Rebelo and J. I. Silva-Marcos, Phys. Rev. Lett. **82**, 683 (1999); E. J. Chun and K. Turzynski, arXiv:hep-ph/0703070.

[4] V. Barger, S. L. Glashow, P. Langacker and D. Marfatia, Phys. Lett. B **540**, 247 (2002); S. Pascoli, S. T. Petcov and W. Rodejohann, Phys. Lett. B **549**, 177 (2002); K. Matsuda, T. Fukuyama and H. Nishiura, Mod. Phys. Lett. A **18**, 1803 (2003); S. Pascoli, S. T. Petcov and T. Schwetz, Nucl. Phys. B **734**, 24 (2006).

[5] S. Blanchet and P. Di Bari, JCAP **0703**, 018 (2007).

[6] A. Dighe, S. Goswami and P. Roy, Phys. Rev. D **73**, 071301(R) (2006).

[7] M. Jezabek and Y. Sumino, Phys. Lett. B **457**, 139 (1999); C. Giunti and M. Tanimoto, Phys. Rev. D **66**, 053013 (2002); Phys. Rev. D **66**, 113006 (2002); P. H. Frampton, S. T. Petcov and W. Rodejohann, Nucl. Phys. B **687**, 31 (2004).

[8] M. Raidal, Phys. Rev. Lett. **93**, 161801 (2004).

[9] H. Minakata and A. Yu. Smirnov, Phys. Rev. D **70**, 073009 (2004); A. Yu. Smirnov, J. Phys. Conf. Ser. **39**, 232 (2006).

[10] P. H. Frampton and R. N. Mohapatra, JHEP **0501**, 025 (2005); S. Antusch, S. F. King and R. N. Mohapatra, Phys. Lett. B **618**, 150 (2005); S. K. Kang, C. S. Kim and J. Lee, Phys. Lett. B **619**, 129 (2005); K. Cheung, S. K. Kang, C. S. Kim and J. Lee, Phys. Rev. D **72**, 036003 (2005); Z.-Z. Xing, Phys. Lett. B **618**, 141 (2005); A. Datta, L. Everett and P. Ramond, Phys. Lett. B **620**, 42 (2005); L. L. Everett, Phys. Rev. D **73**, 013011 (2006); A. Ghosal and D. Majumdar, Mod. Phys. Lett. A **21**, 1067 (2006); A. S. Joshipura and A. Yu. Smirnov, Nucl. Phys. B **750**, 28 (2006).

[11] J. Ferrandis and S. Pakvasa, Phys. Rev. D **71**, 033004 (2005).

[12] P. F. Harrison, D. H. Perkins and W. G. Scott, Phys. Lett. B **458**, 79 (1999); P. F. Harrison, D. H. Perkins and W. G. Scott, Phys. Lett. B **530**, 167 (2002).

[13] F. Vissani, arXiv:hep-ph/9708483; V. D. Barger, S. Pakvasa, T. J. Weiler and K. Whisnant, Phys. Lett. B **437**, 107 (1998); A. J. Baltz, A. S. Goldhaber and M. Goldhaber, Phys. Rev. Lett. **81**, 5730 (1998); G. Altarelli and F. Feruglio, Phys. Lett. B **439**, 112 (1998); M. Jezabek and Y. Sumino, Phys. Lett. B **440**, 327 (1998); D. V. Ahluwalia, Mod. Phys. Lett. A **13**, 2249 (1998).

[14] C. S. Lam, Phys. Lett. B **507**, 214 (2001); P. F. Harrison and W. G. Scott, Phys. Lett. B **547**, 219 (2002).

[15] S. Choubey and W. Rodejohann, Eur. Phys. J. C **40**, 259 (2005); T. Ota and W. Rodejohann, Phys. Lett. B **639**, 322 (2006).

[16] R. N. Mohapatra and S. Nussinov, Phys. Lett. B **441**, 299 (1998).

[17] E. Ma and G. Rajasekaran, Phys. Rev. D **64**, 113012 (2001); E. Ma, Mod. Phys. Lett. A **20**, 2601 (2005); K. S. Babu, E. Ma and J. W. F. Valle, Phys. Lett. B **552**, 207 (2003); G. Altarelli and F. Feruglio, Nucl. Phys. B **741**, 215 (2006); R. R. Volkas, arXiv:hep-ph/0612296.

[18] P. F. Harrison and W. G. Scott, Phys. Lett. B **557**, 76 (2003); W. Grimus and L. Lavoura, JHEP **0508**, 013 (2005); N. Haba, A. Watanabe and K. Yoshioka, Phys. Rev. Lett. **97**, 041601 (2006); R. N. Mohapatra, S. Nasri and H. B. Yu, Phys. Lett. B **639**, 318 (2006).

[19] P. Minkowski, Phys. Lett. B **67**, 421 (1977); T. Yanagida, *Proceedings of the Workshop on the Unified Theory and the Baryon Number in the Universe* (O. Sawada and A. Sugamoto, eds.), KEK, Tsukuba, Japan, 1979, pp 95; M. Gell-Mann, P. Ramond, and R. Slansky, *Supergravity* (P. van Nieuwenhuizen and D. Z. Freedman, eds.), North Holland, Amsterdam, 1979, pp 315; S. L. Glashow, *Proceedings of the 1979 Cargèse Summer Institute on Quarks and Leptons*

(M. Lévy, J.-L. Basdevant, D. Speiser, J. Weyers, R. Gastmans, and M. Jacob, eds.), Plenum Press, New York, 1980, pp. 687; R. N. Mohapatra and G. Senjanovic, Phys. Rev. Lett. **44**, 912 (1980).

[20] R. N. Mohapatra, N. Setzer and S. Spinner, Phys. Rev. D **73**, 075001 (2006).

[21] W. Buchmuller, P. Di Bari and M. Plumacher, Nucl. Phys. B **665**, 445 (2003).

[22] K. S. Babu, C. N. Leung and J. T. Pantaleone, Phys. Lett. B **319**, 191 (1993); M. Tanimoto, Phys. Lett. B **360**, 41 (1995); J. A. Casas, J. R. Espinosa, A. Ibarra and I. Navarro, Nucl. Phys. B **569**, 82 (2000); K. R. S. Balaji, A. S. Dighe, R. N. Mohapatra and M. K. Parida, Phys. Rev. Lett. **84**, 5034 (2000); Phys. Lett. B **481**, 33 (2000); N. Haba, Y. Matsui and N. Okamura, Eur. Phys. J. C **17**, 513 (2000); S. Antusch, M. Drees, J. Kersten, M. Lindner and M. Ratz, Phys. Lett. B **519**, 238 (2001); Phys. Lett. B **525**, 130 (2002); T. Fukuyama and N. Okada, JHEP **0211**, 011 (2002); G. Bhattacharyya, A. Raychaudhuri and A. Sil, Phys. Rev. D **67**, 073004 (2003); A. S. Joshipura, S. D. Rindani and N. N. Singh, Nucl. Phys. B **660**, 362 (2003); R. N. Mohapatra, M. K. Parida and G. Rajasekaran, Phys. Rev. D **69**, 053007 (2004).

[23] J. A. Casas, J. R. Espinosa, A. Ibarra and I. Navarro, Nucl. Phys. B **573**, 652 (2000).

[24] S. Antusch, J. Kersten, M. Lindner and M. Ratz, Nucl. Phys. B **674**, 401 (2003).

[25] M. Drees, R. Godbole and P. Roy, "Theory and phenomenology of sparticles," *Hackensack, USA: World Scientific (2004).*

[26] M. A. Schmidt and A. Yu. Smirnov, Phys. Rev. D **74**, 113003 (2006).

[27] S. Luo and Z. Z. Xing, Phys. Lett. B **632**, 341 (2006).

[28] Particle Data group, W.-M. Yao *et al.*, Journal of Physics G 33, 1 (2006).

[29] A. Strumia and F. Vissani, Nucl. Phys. B **726**, 294 (2005); B. Aharmim *et al.* [SNO Collaboration], Phys. Rev. C **72**, 055502 (2005); S. Goswami, Int. J. Mod. Phys. A **21**, 1901 (2006); G. L. Fogli, E. Lisi, A. Marrone and A. Palazzo, Prog. Part. Nucl. Phys. **57**, 742 (2006); T. Schwetz, Phys. Scripta **T127**, 1 (2006).

[30] J. W. Mei and Z. Z. Xing, Phys. Rev. D **70**, 053002 (2004); R. N. Mohapatra, M. K. Parida and G. Rajasekaran, Phys. Rev. D **71**, 057301 (2005); J. R. Ellis, A. Hektor, M. Kadastik, K. Kannike and M. Raidal, Phys. Lett. B **631**, 32 (2005); S. K. Kang, C. S. Kim and J. Lee, Phys. Lett. B **619**, 129 (2005); S. T. Petcov, T. Shindou and Y. Takanishi, Nucl. Phys. B **738**, 219 (2006).

[31] H. Arason, D. J. Castano, E. J. Piard and P. Ramond, Phys. Rev. D **47**, 232 (1993).

[32] P. H. Chankowski and S. Pokorski, Int. J. Mod. Phys. A **17**, 575 (2002).

[33] J. R. Ellis and S. Lola, Phys. Lett. B **458**, 310 (1999); P. H. Chankowski, W. Krolikowski and S. Pokorski, Phys. Lett. B **473**, 109 (2000).

[34] S. F. King, JHEP **0508**, 105 (2005).

[35] F. Plentinger and W. Rodejohann, Phys. Lett. B **625**, 264 (2005).

[36] H. Georgi and C. Jarlskog, Phys. Lett. B **86**, 297 (1979).

[37] R. Barbieri, J. R. Ellis and M. K. Gaillard, Phys. Lett. B **90**, 249 (1980); E. K. Akhmedov, Z. G. Berezhiani and G. Senjanovic, Phys. Rev. Lett. **69**, 3013 (1992); E. K. Akhmedov, Z. G. Berezhiani, G. Senjanovic and Z. J. Tao, Phys. Rev. D **47**, 3245 (1993); A. S. Joshipura, Phys. Rev. D **60**, 053002 (1999); A. de Gouvea and J. W. F. Valle, Phys. Lett. B **501**, 115 (2001); F. Vissani, M. Narayan and V. Berezinsky, Phys. Lett. B **571**, 209 (2003); B. S. Koranga, M. Narayan and S. U. Sankar, hep-ph/0611186.

[38] A. Dighe, S. Goswami and W. Rodejohann, Phys. Rev. D **75**, 073023 (2007).

[39] F. Ardellier *et al.* [Double Chooz Collaboration], arXiv:hep-ex/0606025; X. Guo *et al.* [Daya Bay Collaboration], arXiv:hep-ex/0701029.

[40] A. Bandyopadhyay, S. Choubey and S. Goswami, Phys. Rev. D **67**, 113011 (2003); H. Minakata, H. Nunokawa, W. J. C. Teves and R. Zukanovich Funchal, Phys. Rev. D **71**, 013005 (2005); A. Bandyopadhyay, S. Choubey, S. Goswami and S. T. Petcov, Phys. Rev. D **72**, 033013 (2005).